Ecological Applications, 21(2), 2011, pp. 477–489

Burn severity influences postfire CO_2 exchange in arctic tundra

Adrian V. Rocha[1] and Gaius R. Shaver

The Ecosystems Center, Marine Biological Laboratory, Woods Hole, Massachusetts 02543 USA

Abstract. Burned landscapes present several challenges to quantifying landscape carbon balance. Fire scars are composed of a mosaic of patches that differ in burn severity, which may influence postfire carbon budgets through damage to vegetation and carbon stocks. We deployed three eddy covariance towers along a burn severity gradient (i.e., severely burned, moderately burned, and unburned tundra) to monitor postfire net ecosystem exchange of CO_2 (NEE) within the large 2007 Anaktuvuk River fire scar in Alaska, USA, during the summer of 2008. Remote sensing data from the MODerate resolution Imaging Spectroradiometer (MODIS) was used to assess the spatial representativeness of the tower sites and parameterize a NEE model that was used to scale tower measurements to the landscape. The tower sites had similar vegetation and reflectance properties prior to the Anaktuvuk River fire and represented the range of surface conditions observed within the fire scar during the 2008 summer. Burn severity influenced a variety of surface properties, including residual organic matter, plant mortality, and vegetation recovery, which in turn determined postfire NEE. Carbon sequestration decreased with increased burn severity and was largely controlled by decreases in canopy photosynthesis. The MODIS two-band enhanced vegetation index (EVI2) monitored the seasonal course of surface greenness and explained 86% of the variability in NEE across the burn severity gradient. We demonstrate that understanding the relationship between burn severity, surface reflectance, and NEE is critical for estimating the overall postfire carbon balance of the Anaktuvuk River fire scar.

Key words: Anaktuvuk River fire, Alaska, USA; burn severity; EVI2 (MODIS two-band enhanced vegetation index); NBR (normalized burn ratio); NEE (net ecosystem exchange of CO_2); tundra; upscaling.

Introduction

There is an increasing need to understand how wildfires influence terrestrial carbon cycling at a variety of spatial and temporal scales. Fire frequency has increased in many areas of the world (Oechel and Vourlitis 1997, Kasischke and Turetsky 2006, Westerling et al. 2006) and created heterogeneous landscapes that vary in disturbance history. Fires clear vegetation and decrease ecosystem carbon stocks over large areas, while successional legacies can influence ecosystem carbon sequestration from decades to centuries (Bond-Lamberty et al. 2004, Goulden et al. 2006, McMillan and Goulden 2008). Ecosystems typically lose carbon early in succession as they recover from fire, and sequester carbon later on as they reach canopy closure (Baldocchi 2008). These successional dynamics, when spread across a landscape with different fire histories, can influence regional carbon budgets and complicate efforts to scale bottom-up measurements of CO_2 flux to larger scales (Litvak et al. 2003, Bond-Lamberty et al. 2007).

Burn severity is a measure of the combustion of ecosystem carbon stocks and is used to assess vegetation damage from fire (Keeley 2009). Burn severity influences a variety of postfire soil and vegetation resources including nutrient concentrations (Neary et al. 1999, Brais et al. 2000), soil physical properties (Dyrness and Norum 1983, Johnstone and Chapin 2006), carbon stocks (Meigs et al. 2009), plant propagules (Rowe 1983, Schimel and Granstrom 1996), and resprouting (Keeley 2006). Consequently, temporal or spatial variation in burn severity may have long-lasting effects on the carbon balance of large areas. For example, increased burn severity associated with climate warming may be altering vegetation composition in the boreal region from an evergreen to deciduous-dominated landscape (Johnstone et al. 2010). It is clear that burn severity impacts a variety of factors that control the carbon balance of ecosystems, but the effect of burn severity on whole ecosystem exchanges of CO_2 or landscape carbon budgets has received little attention.

Scaling the impact of burn severity on landscape carbon balance is difficult because of the spatial heterogeneity within burn scars. Burned landscapes are often composed of a mosaic of patches that differ in burn severity, which arise from differences in terrain, fuel moisture, vegetation type, or prevailing weather conditions during fire (Kasischke et al. 2000, Duffy et al. 2007). These patches likely differ in CO_2 exchange, and observations from a single site are unlikely to be representative of the entire fire scar. Furthermore, extrapolating CO_2 fluxes to larger spatial scales may

Manuscript received 4 February 2010; revised 22 April 2010; accepted 26 April 2010. Corresponding Editor: K. K. Treseder.

[1] E-mail: arocha@mbl.edu

result in large biases if spatial variability in surface conditions is poorly represented (Quaife et al. 2008, Stoy et al. 2009*b*). Remote sensing observations capture spatial variability in surface conditions and have been combined with CO_2 flux data measured by eddy covariance tower networks to improve carbon balance estimates of large regions (Jung et al. 2008, Xiao et al. 2008). It is unclear, however, if remote sensing observations could be used to improve postfire carbon balance estimates from burned landscapes.

The Anaktuvuk River fire burned 1039 km^2 of arctic tundra from July to October 2007 and created a mosaic of large patches that differed in burn severity (Jones et al. 2009). The fire was the largest ever recorded on the North Slope of Alaska and provided a unique opportunity to investigate the effect of burn severity on ecosystem carbon balance. Three eddy covariance towers were deployed within the Anaktuvuk River fire scar during the summer of 2008 to monitor the net ecosystem exchange of CO_2 (NEE) along a burn severity gradient (i.e., severely, moderately, and unburned tundra). Observations of the two-band enhanced vegetation index (EVI2) and the normalized burn ratio (NBR) from the Moderate Resolution Imaging Spectroradiometer (MODIS) were used to assess the spatial and temporal representativeness of the tower sites and validate our experimental approach. We also determined the sensitivity of the landscape carbon balance to burn severity by developing a NEE model using EVI2 observations from each site, and scaled this relationship using EVI2 maps of the Anaktuvuk River burn scar. We hypothesized that burn severity determines the postfire carbon balance of the Anaktuvuk River fire scar by influencing NEE through damage to vegetation and carbon stocks.

Methods

Experimental setup

We deployed three eddy covariance towers with identical instrumentation across a burn severity gradient (Rocha and Shaver 2009). The three sites (i.e., the Severe burn, Moderate burn, and Unburned sites) were located 40 km to the west of the nearest road and selected during a helicopter survey of the southern area of the Anaktuvuk River fire scar in late May 2008 (Fig. 1, Table 1). Because the fire had burned through September of the previous year, deployment of flux towers occurred prior to any significant vegetative regrowth, and our sampling campaign captured the full 2008 growing season (1 June–28 August). Each site was equipped with a Campbell Scientific CR5000 datalogger that recorded data from micrometeorological instrumentation located on a stainless steel tripod (CM110; Campbell Scientific, Logan Utah, USA) at a height of 2.6 m. Data were stored on a 2-Gb PCMCIA card and downloaded every 2–3 weeks. Power for the datalogger and instrumentation was located 15 m to the east or west of the tower and consisted of a south-facing solar panel and two 12-V 80 ampere-hour batteries enclosed in a polyethylene box. Towers ran continuously through the summer of 2008 with the exception of the Severe burn site, which was damaged by a bear during the last week of August.

Environmental data were recorded as half-hour averages. Net radiation was monitored with a NRLITE net radiometer (Campbell Scientific, Logan Utah, USA). Incoming and reflected solar and longwave radiation were measured with a CNR-1 Radiometer (Campbell Scientific), while incoming and reflected photosynthetically active radiation (PAR) were measured with a silicon quantum sensor (LI-COR, Lincoln, Nebraska, USA). Air temperature and relative humidity were measured with an HMP45C-L sensor (Campbell Scientific) enclosed in a naturally aspirated radiation shield, while precipitation was measured with a tipping bucket rain gauge (TE525; Campbell Scientific). Volumetric water content at a depth of 2.5 cm was measured with two reflectometers (CS616; Campbell Scientific), soil temperatures at depths of 2 and 6 cm were measured with two averaging soil thermocouples (TCAV-L; Campbell Scientific), and soil heat flux at a depth of 8 cm was measured with four soil heat flux plates (HFP01; Campbell Scientific). Soil sensors were installed in late June of 2008 after soil thaw depths were $>$10 cm. Measurements of the soil environment were recorded on the CR5000 datalogger at the Unburned site and on separate CR1000 dataloggers at the Severe and Moderate burn sites.

Turbulent fluxes of momentum, sensible heat, latent heat, and CO_2 were determined by the eddy covariance technique (Baldocchi et al. 1988). Half-hourly CO_2 and H_2O fluxes were calculated as the covariance between the turbulent departures from the mean of the 10-Hz vertical wind speed measured with a 3-D sonic anemometer (CSAT3; Campbell Scientific) and the CO_2 and H_2O mixing ratio measured with an open path infrared gas analyzer (IRGA, LI7500; LI-COR). Fluxes were processed using EdiRe software (University of Edinburgh [Moncrieff et al. 1997]) and reported using the meteorological sign convention where negative NEE indicates carbon uptake and positive NEE indicates carbon loss from the ecosystem. Ten-Hz data were despiked, rotated to the mean wind streamlines, and corrected for the density effect due to sensible heat transfer (i.e., WPL correction [Webb et al. 1980]). Turbulent fluxes of sensible and latent heat captured 78–80% of the available energy at each of the sites, which is consistent with energy budget closure observed for other eddy covariance studies (Wilson et al. 2002).

Cumulative sums and sources of error

Quality of CO_2 flux data depended on adequate turbulent mixing and instrument functioning. Adequate turbulent mixing, as determined from plots of NEE with $PAR_i < 20$ $\mu mol \cdot m^{-2} \cdot s^{-1}$ vs. friction velocity (u^*), occurred for $u^* > 0.10$ m/s. Diagnostic flags for the

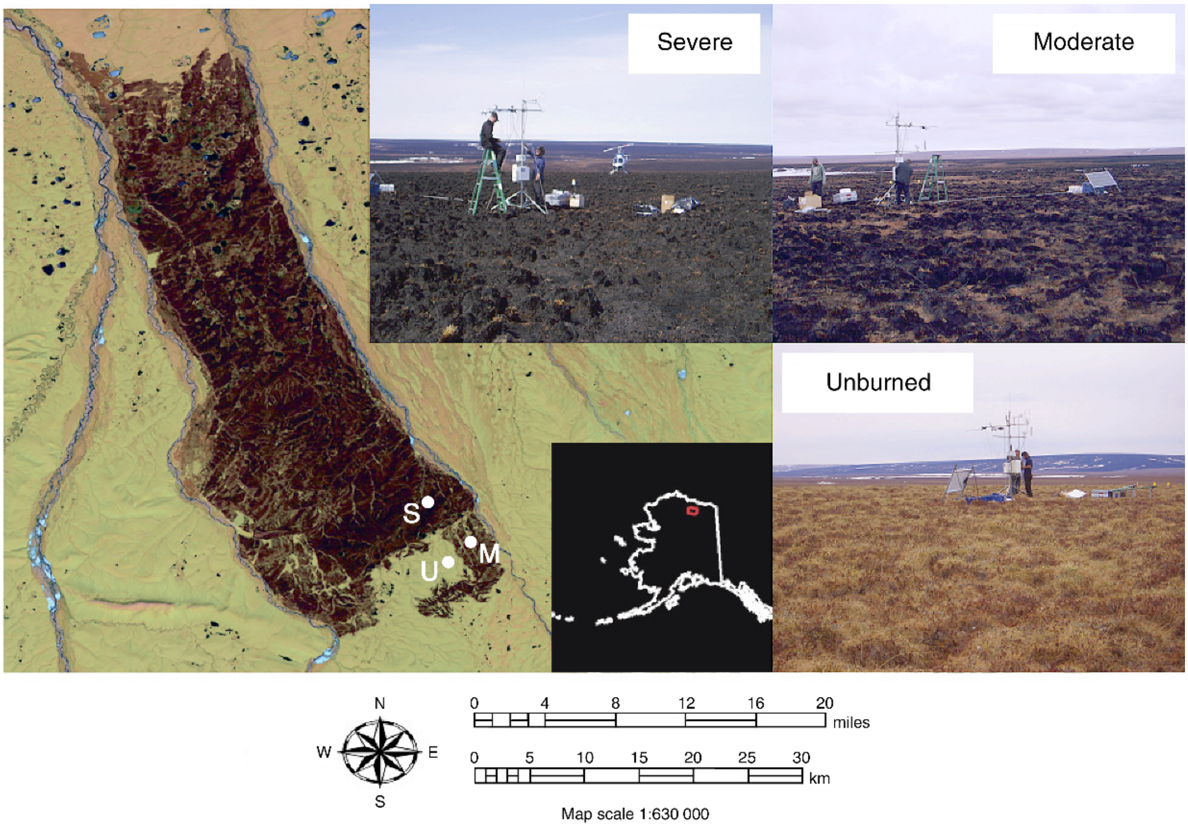

FIG. 1. Landsat false color image of the Anaktuvuk River fire scar in July of 2008 with the location of the Severe (S), Moderate (M), and Unburned (U) sites indicated with white circles. The red square on the map of Alaska, USA, shows the location of the Anaktuvuk River fire scar. Site photographs were taken during the first week of June 2008. Photo credits: Jim Laundre and Gus Shaver.

TABLE 1. Description of study sites in the Anaktuvuk River burn scar, Alaska, USA.

Site	Location	Prefire summer EVI2† (mean and 95% CI)	Conditions after first growing season
Severe burn	68°59′4″ N, 150°16′52″ W	0.37 ± 0.01	Largely absent moss layer (<5% of ground cover) with mineral soil exposed in 10% of area surrounding tower. Recovering and dead tussocks [*Eriophorum* spp.] formed the dominant canopy cover with burned duff (60% of ground cover) and sparse vegetation (cloudberry [*Rubus chamaemorus* L.], Labrador tea [*Ledum palustre* L.]) comprising the intertussock area. Of the scorched tussocks, 70% resprouted after the first growing season.
Moderate burn	68°57′08″ N, 150°12′43″ W	0.37 ± 0.01	A mosaic of partially and completely burnt moss patches scattered across the landscape that varied in size from ~1 to 10 m^2. Partially burnt moss cover was 33% and dominated by sphagnum [*Sphagnum* spp.] and feather mosses [*Hylocomium* spp.]. Recovering and dead tussocks formed the dominant canopy cover. Intertussock area was composed of burnt duff (30% of ground cover) and several herbaceous species (cloudberry; Labrador tea, and cranberry [*Vaccinium vitis-idaea* L.]). Of the scorched tussocks, 95% resprouted after the first growing season.
Unburned	68°56′04″ N, 150°16′22″ W	0.38 ± 0.01	Unburned tussock tundra vegetation community with 40% of the ground covered with sphagnum and feather mosses, and the remaining ground cover composed of tussocks, cloudberry, Labrador tea, cranberry, and dwarf birch [*Betula nana* L.].

† EVI2 is enhanced vegetation index 2.

IRGA and sonic anemometer were recorded by the datalogger and used to identify improper instrument functioning. NEE data during periods with inadequate turbulent mixing or periods with instrument malfunction were excluded from the analysis, and the remaining flux data set was referred to as "unfilled" NEE. Unfilled data represented 61% of the NEE record from the Severe burn, 64% of the NEE record from the Moderate burn, and 62% of the NEE record from the Unburned site. Gaps in the NEE time series were filled using weekly parameterized light response curves with unfilled NEE and incoming PAR data (PAR_i) in order to calculate cumulative sums (Ruimy et al. 1995):

$$NEE = R - \frac{NEE_{max} PAR_i}{K_0 + PAR_i}. \quad (1)$$

Least-squares regressions were used with Eq. 1 to determine weekly ecosystem respiration (R) (i.e., the y-intercept of the light response curve), light-saturated NEE (NEE_{max}), and the photosynthetic compensation point (K_0) at each site. Parameters from the light response curves also were used to determine how carbon uptake and loss differed across the burn severity gradient. Since the 24-hour arctic summer photoperiod makes partitioning NEE into photosynthesis and respiration difficult, we used the weekly estimates of R (Eq. 1) as a measure of ecosystem respiration and NEE_{max} as a measure of weekly maximum canopy net photosynthesis. Analysis of variance (ANOVA) and Tukey-Kramer comparisons were used to determine statistical differences in NEE_{max} and R among sites at the 95% confidence level.

Measurement of NEE with open or closed path sensors presents a trade-off between power usage and accuracy. Open-path sensors are ideal for operation at remote field sites because they require substantially less power and maintain calibration longer than closed-path sensors, but can overestimate carbon uptake during cold periods (Burba et al. 2008). Correction factors based on empirical relationships between air temperature, outgoing longwave radiation, and wind speed have been developed to account for the overestimation of carbon uptake during cold periods (Burba et al. 2008; herein referred to as the "Burba correction"), but the robustness of the Burba correction has not been thoroughly assessed or adopted yet by tower flux networks, such as Ameriflux.

We calculated the uncertainty in the cumulative NEE at the three sites by incorporating measurement error from open path instrumentation. We applied the two empirical formulations in Burba et al. (2008) with air temperature only (Method 1) and with air temperature, wind speed, and outgoing longwave radiation (Method 2). The Burba corrections had little effect on the absolute differences in cumulative NEE among sites along the burn severity gradient, but resulted in less carbon uptake at each site, with Method 1 resulting in the least amount of carbon uptake. We analyzed NEE with and without the Burba correction to validate the robustness of our conclusions, and used the average NEE between the Burba corrected (Methods 1 and 2) and uncorrected methods as our best estimate of cumulative NEE, where the range represented measurement uncertainty. NEE data presented in the graphs are not Burba corrected, so that direct comparison with previous open-path studies can be made.

Remote sensing data

We used the 500-m-resolution eight-day MODIS surface reflectance composite images from the Terra satellite (MOD09A1) to assess differences in surface greenness and burn severity across the Anaktuvuk River fire scar during the 2008 summer (day of year: 161–241). Ten MODIS images were obtained in Hierarchical Data Format (HDF) and reprojected to geographic latitude/longitude in ENVI (ITT Visual Information Solutions, Boulder, Colorado, USA). We used EVI2 as a measure of surface greenness because it is less sensitive to atmospheric aerosols and soil reflectance than the more commonly used Normalized Difference Vegetation Index (Jiang et al. 2008, Rocha and Shaver 2009). EVI2 is functionally equivalent to the commonly used three-band EVI across the Anaktuvuk River fire scar ($R^2 = 0.99$; $P < 0.001$; RSME = 0.003; $n = 46610$; also see Rocha and Shaver 2009), but it only incorporates the Near InfraRed ($\rho_{NIR} = 841–876$ nm; MODIS Band 2) and Red (ρ_{RED}: 620–670 nm; MODIS Band 1) reflectance (Eq. 2, below). The normalized burn ratio (NBR) was used as a proxy for burn severity and incorporated reflectance in the NIR and ShortWave InfraRed (ρ_{SWIR}: 1230–1250 nm; MODIS Band 5; Key and Benson 1999) (Eq. 3):

$$EVI2 = 2.5 \frac{\rho_{NIR} - \rho_{RED}}{\rho_{NIR} + 2.4\rho_{RED} + 1} \quad (2)$$

$$NBR = \frac{\rho_{NIR} - \rho_{SWIR}}{\rho_{NIR} + \rho_{SWIR}}. \quad (3)$$

We extracted a seasonal time series of EVI2, as well as the initial normalized burn ratio (NBR) (day of year =161, 2008; day 1 is 1 January) for a 1-km^2 area centered on each tower site (Rocha and Shaver 2009) and for each pixel within the Anaktuvuk River burn scar in 2008. The perimeter of the Anaktuvuk River burn scar was detected using the initial NBR image, and traced using the Region Of Interest (ROI) tool in ENVI. Lake-covered pixels were identified by consistent negative EVI2 throughout the summer and comprised <1% of the total area, while cloudy pixels were identified using a reflectance threshold of 10% on the blue reflectance and comprised 4% of the EVI2 data set. Pixels with short gaps (i.e., 1 eight-day period) caused by clouds were filled by averaging EVI2s from the date prior to and after the missing period, while pixels with larger gaps (>1 eight-day period) represented <0.5% of the EVI2 data set and were omitted from subsequent analyses due to the difficulty in filling large gaps.

MODIS data also were used to assess the spatial and temporal representativeness of the tower sites. Prefire summer (DOY: 161–241) MODIS EVI2 from 2000 to 2006 was obtained for each tower site and used to determine how well the sites were matched prior to the Anaktuvuk River fire. Average summer EVI2 in 2008 represented an integrated proxy of surface conditions and was used to determine the spatial representativeness of the tower sites in comparison with the average 2008 summer EVI2s observed within the Anaktuvuk River fire scar.

Ground-based biometric data

Ground-based assessments of burn severity and vegetation recovery were undertaken within the fetch of each eddy covariance tower. We recorded tussock mortality, percentage of unburned moss, and mineral soil cover, and dominant species at each site in 30 1-m^2 quadrats in late May of 2009. We compared the MODIS two-band enhanced vegetation index (EVI2) with ground-based EVI2 derived from radiative fluxes measured with tower instrumentation (Rocha and Shaver 2009) to determine if there was a mismatch between tower and satellite (i.e., MODIS) data. Comparison of MODIS NBR with ground-based measures could not be accomplished because of the difficulty in extracting ρ_{SWIR} from ground-based broadband radiation measurements.

Model development and scaling exercise

Our goal was to develop a simple empirical model from MODIS EVI2 and NEE data to determine how burn severity influenced estimates of postfire summer carbon balance in 2008. Model development was undertaken using multiple linear regression with averaged eight-day daily NEE as the explanatory variable and eight-day MODIS EVI2, averaged eight-day temperature, and integrated eight-day PAR_i at each site as predictor variables. Tower measurements were then scaled to the Anaktuvuk River fire scar (NEE_{act}; actual net ecosystem exchange) using the empirical model and MODIS EVI2 images during the summer of 2008.

To determine the effect of burn severity on the carbon balance of the entire fire scar, we assumed that the probability distribution of burn severity and EVI2 were similar and determined how changes in the probability distribution affected summer carbon balance estimates. We represented the spatial distribution of burn severity within the Anaktuvuk River fire scar using a binomial probability distribution (Shelby 1969), and calculated the carbon balance using the derived empirical model for 101 distributions that differed in skewness (NEE_{est}; estimated net ecosystem exchange). We calculated the difference between NEE_{est} and NEE_{act} ($NEE_D = NEE_{est} - NEE_{act}$) and plotted them against skewness to determine how changes in burn severity influence carbon balance estimates. The range of the binomial distributions was constrained to EVI2s that were observed within the burn scar. A negative skewness indicated a fire scar with a lower burn severity than observed, while a positive skewness indicated a fire scar with a higher burn severity than observed. NEE_D was expressed in grams of carbon per square meter, and represented a spatially averaged difference across the Anaktuvuk River fire scar. A negative NEE_D indicated that the probability distribution produced a summer carbon balance that sequestered more carbon than observed, while a positive NEE_D indicated that the probability distribution produced a summer carbon balance that lost more carbon than observed. The range of NEE_D was compared to the year-to-year summer NEE variability reported in Kwon et al. (2006) and Lafleur and Humphreys (2008) for arctic tussock tundra.

Results

Environmental conditions

Environmental conditions at the tower sites were similar during the 2008 summer with the exception of soil temperature (Fig. 2). Daily integrated PAR (ANOVA; $F_{2,246} = 0.06$; $P = 0.94$) (Fig. 2A) and daily average air temperature (ANOVA; $F_{2,246} = 0.11$; $P = 0.90$) (Fig. 2B) were not statistically different among sites, peaking in late June and then decreasing through July and August. Soil temperatures significantly differed among sites (ANOVA; $F_{2,246} = 7086$; $P < 0.001$), and were 53% higher than the Unburned site at the Severe burn and 42% higher than the Unburned site at the Moderate burn (Fig. 2C). Environmental conditions in 2008 at the nearby Toolik Lake Long Term Ecological Research Station were similar to the averages over the past two decades (1988–2008), with average summer temperature 15% lower, cumulative summer PAR 1% higher, and cumulative summer precipitation 14% higher than the historical average.

Pre- and postfire site conditions

Tower sites were well matched before the burn and represented contrasting burn severities following the fire. Prefire EVI2 was not statistically different among the three sites ($F_{2,138} = 0.09$; $P = 0.91$) (Table 1), while plant mortality, residual organic matter, and species composition differed substantially following fire. The Severe burn had exposed mineral soils in 10% of the area, and charred tussocks, while the Moderate burn consisted of a mosaic of partially to completely burned patches of tundra that varied in size from 1 to 10 m^2. Moss cover constituted 5% of the area at the Severe burn and 33% of the area at the Moderate burn. Recovering vegetation at the burned sites consisted of *Eriophorum* tussocks and herbaceous forbs (cloudberry; *Rubus chamaemorus* L.) within the intertussock areas. Tussock mortality differed among burn sites and was 30% at the Severe burn and 5% at the Moderate burn.

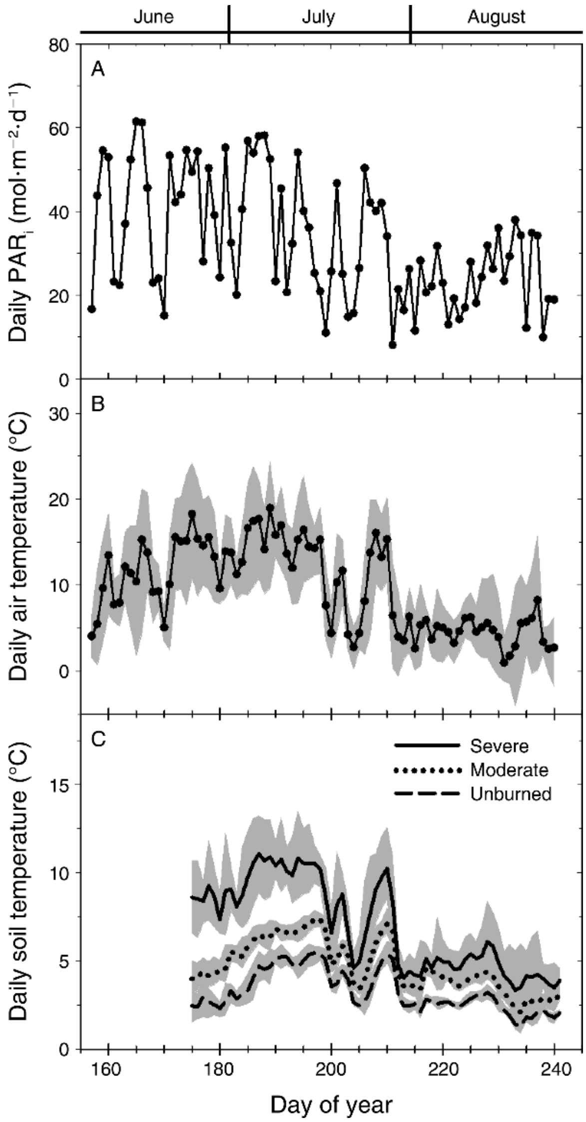

FIG. 2. (A) Daily incoming photosynthetically active radiation (PAR$_i$), (B) daily average air temperature, and (C) daily average soil temperature in the Anaktuvuk River fire scar in Alaska, USA, during the summer of 2008. PAR$_i$ and daily average temperatures represent averages from the three sites, while the gray area represents the average diel temperature range. Day 1 is 1 January.

Differences in the vegetation and organic matter consumed in the fire influenced surface reflectance. Initial MODIS normalized burn ratio (NBR) differed significantly across sites (ANOVA, $F_{2,9} = 159$; $P < 0.001$), and was lowest at the Severe burn and highest at the Unburned site (Fig. 3A). Initial MODIS EVI2 and NBR were positively correlated across the entire burn scar ($R^2 = 0.87$; $P < 0.001$; $n = 4628$), and patterns in initial EVI2 among sites followed those observed for NBR (ANOVA; $F_{2,9} = 507$; $P < 0.001$) (Fig. 3B). Both remote and tower-based measures of EVI2 captured differences across the burn severity gradient with low initial EVI2 at the Severe burn and high initial EVI2 at the Unburned site.

Tower site representativeness

Average summer EVI2 at the tower sites represented the observed range across the Anaktuvuk River fire scar (Fig. 4). Average summer EVI2s were positively skewed and reflected the high severity of the fire (Jones et al. 2009). Tower sites spanned the range of burn severities with the Severe burn in the 14th to 58th percentile, the Moderate burn in the 86th to 96th percentile, and the Unburned in the 99th to 100th percentile of the average summer EVI2 distribution.

Burn severity and CO_2 exchange

Burn severity influenced the magnitude and the daily and seasonal changes of the net ecosystem exchange of CO_2 (NEE) (Fig. 5). Diel NEE variability across the burn severity gradient tracked light availability, and was lowest during the middle of the day. Seasonal NEE changes followed vegetation phenology and recovery of leaf area (Rocha and Shaver 2009), but differed among sites in its magnitude and timing. The number of days

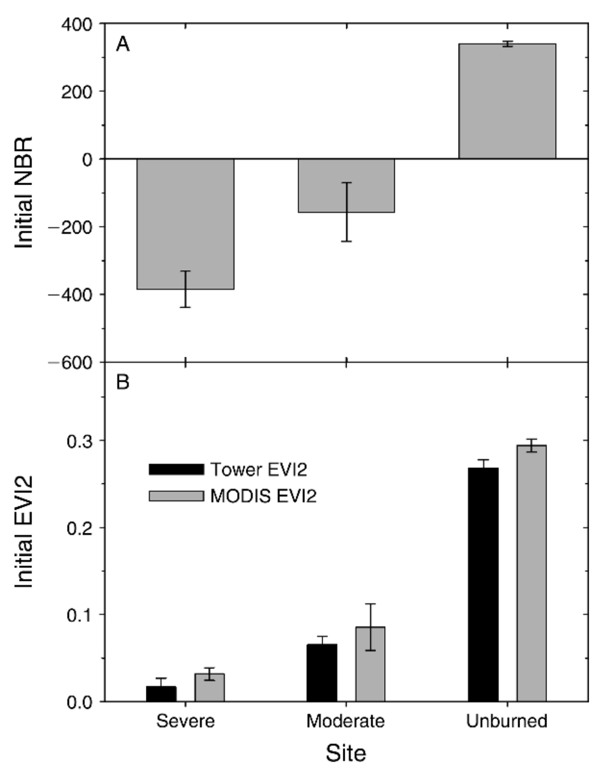

FIG. 3. (A) Initial (day of year, 157–165) MODIS normalized burn ratio (NBR) and (B) the initial two-band enhanced vegetation index (EVI2) measured by MODIS (gray bars) and ground-based radiative fluxes (black bars) across the burn severity gradient. See *Remote sensing data*, Eqs. 2 and 3, for the calculation of NBR and EVI2. Error bars represent 95% confidence intervals.

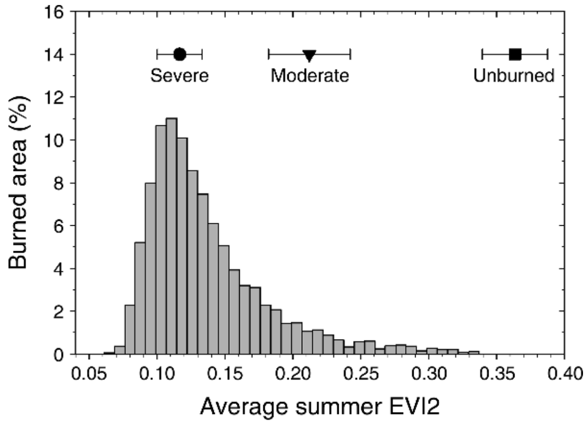

FIG. 4. Probability distribution of the averaged summer (day of year, 161–241) two-band enhanced vegetation index (EVI2) across the Anaktuvuk River burn scar along with the average summer EVI2 at the Severe, Moderate, and Unburned sites during the summer of 2008. Error bars represent 95% confidence intervals.

with negative midday NEE was 73 days shorter at the Severe burn and 38 days shorter at the Moderate burn than observed at the Unburned site. The lowest NEE occurred in early July at the Unburned site, and in early to mid-August at the burned sites.

Comparison of the light response curve parameters among sites reveals how respiratory carbon losses and photosynthetic carbon gains varied along the burn severity gradient (Fig. 6). NEE_{max} (expressed as a positive value in Fig. 6) represented photosynthetic carbon gain and significantly differed among sites (ANOVA, $F_{2,38} = 5.56$; $P < 0.01$), whereas R represented respiratory carbon loss and was not significantly different among sites (ANOVA, $F_{2,38} = 0.48$; $P = 0.63$). NEE_{max} was lowest at the Severe burn and highest at the Unburned site, and differences in NEE_{max} along the burn severity gradient were 89% larger than observed for R.

Differences in the phase of the seasonal NEE cycle and carbon uptake altered summer carbon balance along the burn severity gradient (Fig. 7). Low photosynthetic rates at the burned sites were insufficient to offset respiratory losses and resulted in increased cumulative NEE during the beginning of the summer. Cumulative NEE at the Unburned site decreased throughout the summer and saturated toward the end of July, while cumulative NEE at the Moderate burn increased until the end of June and then leveled off when photosynthetic carbon gains offset respiratory losses. Cumulative NEE at the Severe burn increased throughout the summer and began to level off at the end of July. For the entire summer, the Severe burn was a carbon source of 110 ± 38 g C/m^2, the Moderate burn was a weak carbon source or sink of 38 ± 40 g C/m^2, and the Unburned site was a carbon sink of 44 ± 38 g C/m^2 (see *Methods: Cumulative sums and sources of error*). By the end of the 2008 summer season the cumulative NEE at the Severe burn was 154 g C/m^2 greater than at the Unburned site, while the difference from the Unburned site was 82 g C/m^2 at the Moderate site.

Controls on NEE across burn severity gradient

Vegetation recovery and phenology, as measured by MODIS EVI2, controlled weekly variations in NEE across the burn severity gradient ($R^2 = 0.86$; $P < 0.001$) (Fig. 8). EVI2 explained 86% of weekly NEE variability across the burn severity gradient, while environmental variables such as temperature and PAR explained <3%. The slope of the EVI2 and NEE relationship varied slightly among sites, but cumulative NEE estimates from the all-sites model resulted in minor errors (Table 2). For example, the RMSE for the all-sites model ranged from 0.24 to 0.37 g C·m^{-2}·d^{-1}, which translated into in a

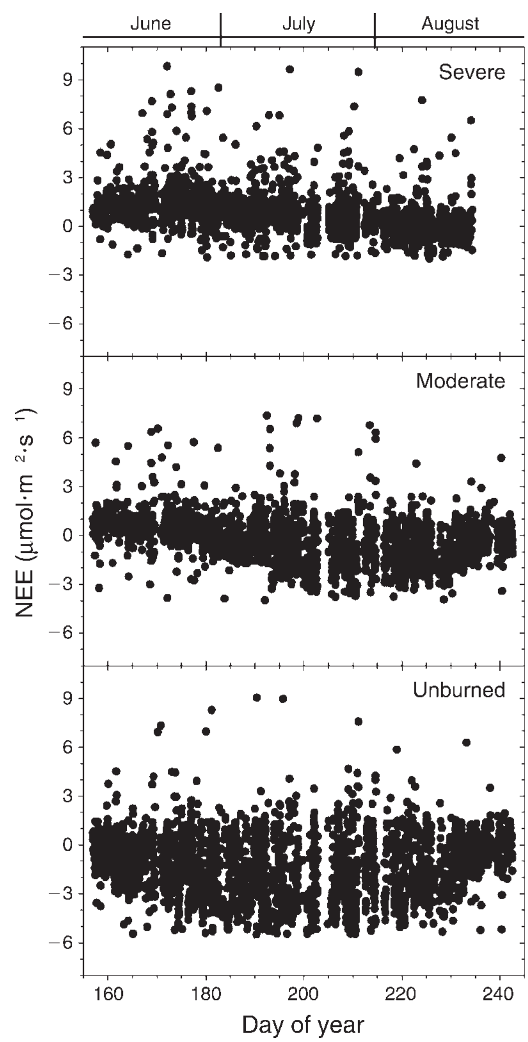

FIG. 5. The net ecosystem exchange of CO_2 (NEE) at the Severe (top panel), Moderate (middle panel), and Unburned sites (bottom panel) during the summer of 2008. Data points are half-hourly average fluxes presented in the atmospheric sign convention, where a positive flux indicates the net transfer of carbon from the ecosystem to the atmosphere.

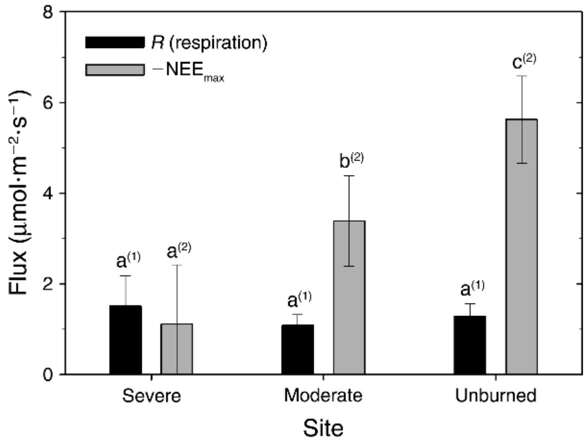

FIG. 6. Average ecosystem respiration (R) (black bars) and light-saturated net ecosystem exchange (NEE_{max}) (gray bars) at the Severe, Moderate, and Unburned sites for the 2008 summer. NEE_{max} is multiplied by -1 for graphical purposes, and higher $-NEE_{max}$ indicates higher rates of carbon uptake. Vertical lines represent 95% confidence intervals, superscript numbers indicate comparisons between R (1) and NEE_{max} (2), and different letters indicate statistical differences ($P < 0.05$).

-0.27 g C/m^2 difference in estimated cumulative summer NEE at the Severe burn, a 1.3 g C/m^2 difference in estimated cumulative summer NEE at the Moderate burn, and a -1.0 g C/m^2 difference in estimated cumulative summer NEE at the Unburned site. The strong dependence of NEE on EVI2 indicates a need to understand the factors that control EVI2 and vegetation recovery. Burn severity controlled the recovery of EVI2 across the fire scar during the first postfire growing season ($R^2 = 0.62$; $P < 0.001$; $n = 4628$) (Fig. 9). Maximum EVI2 during the summer of 2008 was used as a proxy for vegetation recovery and was positively related to initial NBR with areas of high burn severity (i.e., more negative NBR) resulting in less maximum surface greenness, leaf area, and carbon uptake than areas of lower burn severity.

Burn severity and the carbon balance

Differences in the probability distribution of burn severity dramatically altered the estimated summer carbon balance for the entire 1039-km^2 fire scar (Fig. 10). For example, the carbon balance of a severely burned fire scar (i.e. right skewed; NEE_{est}) resulted in a difference (i.e., $NEE_D = NEE_{est} - NEE_{act}$) of 57 g C/m^2 in summer carbon balance estimates, while the carbon balance of a low-severity to unburned fire scar (i.e., left skewed) resulted in a difference of -110 g C/m^2 in summer carbon balance estimates. The sensitivity of carbon balance estimates was highest between the two extremes (i.e., severely burned and unburned fire scar) with a 29 g C/m^2 difference occurring with a 0.1 change in skewness, or a -63 g C/m^2 difference occurring with a 0.1 change in average summer EVI2. Interannual summer NEE variability for tussock tundra was 29 g C·m^{-2}·summer^{-1} over three years (Lafleur and Humphreys 2008) and 32 g C·m^{-2}·summer^{-1} over five years (Kwon et al. 2006). Consequently, the variability in the summer carbon balance associated with burn severity was much larger than year-to-year NEE variability observed for arctic tundra.

DISCUSSION

Multiple eddy covariance towers can be used to understand how NEE varies along ecological and environmental gradients provided that tower sites are well matched in terms of their vegetation and soils and experience similar environmental conditions (Goulden et al. 2006, Rocha and Goulden 2010). In this study, environmental drivers (i.e., air temperature and PAR_i),

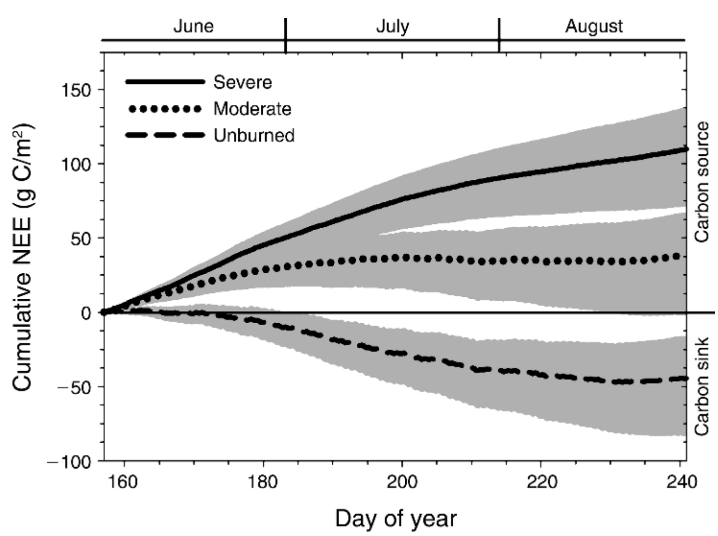

FIG. 7. Cumulative NEE at the Severe (solid line), Moderate (dotted line), and Unburned (dashed line) sites during the 2008 summer. Negative NEE indicates carbon uptake, and positive NEE indicates carbon loss from the ecosystem (see *Methods: Experimental setup*). The gray area represents measurement uncertainty.

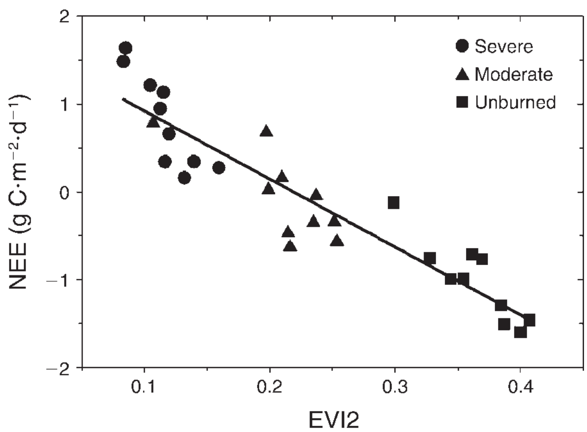

FIG. 8. The relationship between the MODIS two-band enhanced vegetation index (EVI2) and eight-day averaged daily net ecosystem exchange (NEE) across the burn severity gradient during the summer of 2008.

TABLE 2. The root mean-square error (RMSE) and the difference in summer cumulative net ecosystem exchange (NEE) from the empirical relationship between EVI2 and MODIS eight-day NEE given in Fig. 8 for each of the tower sites.

Site	All-sites model RMSE ($g\ C \cdot m^{-2} \cdot d^{-1}$)	Cumulative summer NEE difference (actual−predicted) ($g\ C/m^2$)
Severe	0.26	0.28
Moderate	0.32	–1.29
Unburned	0.16	1.01

prefire EVI2, and vegetation and soil type were all similar among sites, ensuring that the observed differences in NEE were caused largely or entirely by burn severity (Table 1, Fig. 2). Assessing the representativeness of the tower sites is critical for scaling carbon budgets to larger areas because the footprint of the three towers covered <1% of the area within the Anaktuvuk River fire scar. Remote sensing captured the spatial variability in surface conditions of the entire 1039-km^2 area, and provided a valuable tool for determining the spatial representativeness of tower sites (Hargrove et al. 2003, Yang et al. 2008). Average summer EVI2 indicated that tower sites were representative of the variability observed within the Anaktuvuk River fire scar (Fig. 4), and provides confidence in our ability to scale NEE to the entire burned area.

Subpixel spatial variability in burn severity may complicate the upscaling of tower measurements to larger areas because spatial variability within the tower footprint may result in a mismatch of scales between tower measures and MODIS data (Kim et al. 2006, Roman et al. 2009). Ground-based radiation and NEE measurements sample fluxes from a similar area (Schmid 1997), and comparisons between MODIS and tower-based EVI2 were used to determine whether tower locations were biased. MODIS EVI2 differed slightly from tower EVI2, but both measures captured spatial differences in surface greenness between sites (Fig. 3). Tower-derived EVI2 was slightly lower than observed with MODIS as noted in previous work (Rocha and Shaver 2009), and resulted from differences in the spectral response of the sensors and the difference between narrowband MODIS EVI2 and broadband tower EVI2. These results indicate that tower and MODIS measurements integrated fluxes from similar areas, and that within-site spatial variability was largely captured by the MODIS pixel.

The decrease in postfire EVI2 and NBR with increased burn severity both reflected differences in the amount of vegetation and organic matter consumed during the fire. NBR is sensitive to surface darkness and has been used to determine burn severity (Key and Benson 1999), while EVI2 is sensitive to surface greenness and has been used to determine canopy leaf area (Rocha and Shaver 2009). Moss cover following fire provides an indication of burn severity in tundra ecosystems because mosses form extensive surface cover and are more flammable than tussocks due to lower water content in dry summers (Wein 1976, Racine et al. 1987; N. T. Boelman, A. V. Rocha, and G. R. Shaver, *unpublished manuscript*). Residual moss cover decreased with increased burn severity, and areas of high burn severity were less green and darker than areas of low burn severity (Fig. 3, Table 1). Consequently, EVI2 and NBR were positively correlated across the Anaktuvuk River burn scar. Future work will investigate the correlation between EVI2 and NBR, and further assess the sensitivity of these

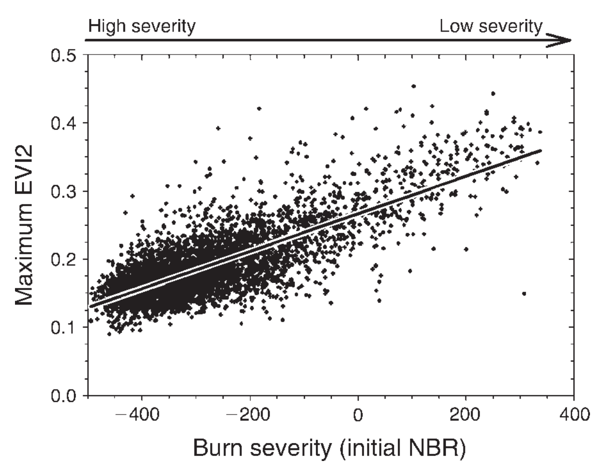

FIG. 9. The relationship between burn severity, as measured by the initial postfire normalized burn ratio (NBR), and vegetation recovery as measured by the maximum two-band enhanced vegetation index (EVI2) during the summer of 2008. Negative NBR indicates areas of high burn severity, while positive NBR indicates areas of low burn severity.

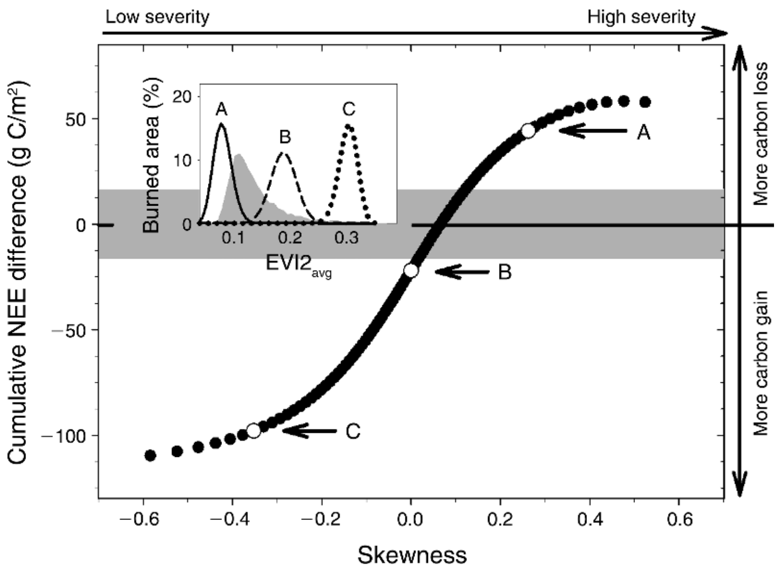

FIG. 10. Cumulative summer net ecosystem exchange differences (NEE_D) as a function of changes in the probability distribution of burn severity across the Anaktuvuk River burn scar. The inset plot shows the original probability distribution of average summer EVI2 ($EVI2_{avg}$) in gray (also see Fig. 4) and the probability distribution of a (solid line A) high-, (dashed line B) moderate-, and (dotted line C) low-severity burn scar. The main plot shows the difference (D) in cumulative summer NEE calculated for each of the altered probability distributions and the actual probability distribution (i.e., NEE_D). Open circles on the curve (i.e., points A, B, and C) in the main plot correspond to NEE_D calculated from the probability distributions located in the inset plot. The gray highlighted area in the main plot represents the reported range of year-to-year cumulative summer NEE variability for tussock tundra (Kwon et al. 2006).

vegetation indices to burn severity within the Anaktuvuk River fire scar (N. T. Boelman, A. V. Rocha, and G. R. Shaver, *unpublished manuscript*).

How did burn severity impact NEE?

Burn severity altered the period of net carbon uptake, maximum carbon uptake, and the seasonality of NEE (Figs. 5, 6, and 7). Net photosynthesis was the dominant controller of NEE variation across the burn severity gradient, and low rates of canopy photosynthesis were unable to offset respiration for a large part of the summer at the burned sites (Figs. 5 and 6). Carbon sequestration in tussock tundra is limited by short growing seasons, and differences in the period of net carbon uptake can have large impacts on carbon sequestration in these systems (Lund et al. 2009). Decreases and shifts in the magnitude and date of peak carbon uptake further exacerbated the effects of burn severity on ecosystem carbon balance. Peak carbon uptake at the burned sites was much lower than in the unburned stand, and occurred in August when low temperatures and light availability could potentially limit NEE (Figs. 2 and 5). Ecosystem respiration did not differ across the burn severity gradient, reflecting the dependence of ecosystem respiration on both biotic and abiotic factors (Davidson et al. 2006). Surface darkening from charred vegetation resulted in increased soil temperatures at the burned sites (Liljedahl et al. 2007, Rocha and Shaver 2009) with no effect on ecosystem respiration (Figs. 2C and 6). Reductions in carbon substrate and changes in the microbial and fungal community as a result of fire can offset increased soil temperatures and result in decreases or no change in soil respiration for several years following fire (Burke et al. 1997, O'Neill et al. 2002, Bergner et al. 2004). The insensitivity of respiration to burn severity implies that NEE was more sensitive to the biotic and abiotic controls of canopy photosynthesis.

What were the controls on NEE across the burn severity gradient?

Diel environmental variability explained a majority of the half-hourly NEE variability, but played less of a role in determining NEE at longer timescales. Half-hourly NEE at each site was mostly controlled by incoming light, while EVI2 controlled weekly NEE across the burn severity gradient (Figs. 5 and 8). EVI2s ability to capture weekly NEE changes across the burn severity gradient without any other environmental information reflected the shift from abiotic to biotic control as NEE is temporally integrated (Richardson et al. 2007, Stoy et al. 2009*a*). EVI2 and NEE are functionally related to canopy leaf area and the photosynthetic potential of arctic plant canopies (Shaver et al. 2007, Lund et al. 2009). Burn severity influenced leaf area recovery in the first postfire growing season, which directly impacted carbon sequestration (Figs. 7 and 9). Recovery of tundra vegetation from fire is dominated by regeneration of tussocks with little seed germination during the first postfire growing season (Wein and Bliss 1973).

Consequently, the high recovery of leaf area at sites of low burn severity was likely driven by low tussock mortality and a higher proportion of unburned tundra patches (Table 1).

How important is burn severity in scaling tower estimates to larger areas?

Burned landscapes present several challenges to quantifying the carbon balance of a fire scar. Burn severity impacted NEE, and as a result, variation in burn severity across the landscape had a significant impact on up-scaled carbon balance estimates (Fig. 10). Classifying the Anaktuvuk River fire as a low-severity burn resulted in an estimated carbon sink during the first postfire growing season, while classifying the Anaktuvuk River fire scar as a high-severity burn resulted in an overestimation of the net carbon loss to the atmosphere during the first postfire growing season. The effect of spatial variation in burn severity on cumulative summer NEE was much greater than the year-to-year variation observed in unburned tundra stands, indicating the importance of burn severity in quantifying the postfire carbon balance of burned landscapes. Bottom-up estimates of terrestrial carbon fluxes are highly dependent on land cover (Quaife et al. 2008), and our results indicate that combining remotely sensed landcover observations with NEE measurements from eddy covariance towers can minimize biases in postfire carbon balance estimates from fire scars.

Although our empirical model did not incorporate meteorological drivers, we believe that our results are robust for several reasons. EVI2 was the first-order controller of NEE across the burn severity gradient, and neglecting environmental drivers in the empirical model resulted in only very small errors in cumulative NEE (Table 2 and Fig. 8). Incorporating meteorological drivers into models driven by remote sensing observations may be redundant, as biotic controls integrate environmental variability over time (Jung et al. 2008). Meteorological drivers may increase the uncertainty in NEE because these data sets are interpolated from a network of meteorological stations and are not truly representative of a single pixel (Jung et al. 2008). Consequently, several studies have encouraged the use of models that solely use remotely sensed vegetation indices to estimate NEE across large areas (Rahman et al. 2005, Jung et al. 2008).

Conclusions

The Anaktuvuk River fire was an unprecedented event that affected ecosystem carbon cycling over 1039 km^2 (Jones et al. 2009). We estimate an overall net carbon loss of 92 $\pm$ 35 Gg C over the entire burn scar during the first summer of recovery following the 2007 fire using the spatially integrated NEE_{act} (see *Methods: Model development and scaling exercise*). This can be compared with a net carbon gain of -51 ± 35 Gg C in a 1039-km^2 unburned area of tundra that is similar to our unburned tower site. Although the Anaktuvuk River burn scar covers only 0.55% of the 188 448-km^2 area of the North Slope (Raynolds et al. 2005), the net release of 92 $\pm$ 35 Gg C would be sufficient to cause a 2.8% decrease in the carbon sink of the entire North Slope in 2008, assuming that the carbon balance of the unburned site is representative of all unburned areas on the North Slope. This is likely to be a conservative estimate, since it assumes an equal carbon balance for the less productive wet sedge areas that take up a large part of the North Slope landscape. It is noteworthy that the percentage change in the North Slope's carbon sink is five times larger than the percentage of the North Slope area that encompasses the Anaktuvuk River fire scar. These results indicate that postfire effects on carbon cycling are important at a variety of spatial scales that range from the ecosystem to region. Consequently, managing the arctic fire regime to minimize both severity and extent is critical in order to reduce postfire carbon losses.

The Arctic is experiencing several kinds of environmental changes that challenge our ability to predict the future carbon balance of high latitudes. Higher temperatures have increased productivity of arctic plants (Goetz et al. 2005, Hudson and Henry 2009), increased shrub abundance (Tape et al. 2006), and created conditions that may be more favorable to lightning strikes (Reeve and Toumi 1999). These changes may favor an increase in arctic wildfires (Higuera et al. 2008), which have major impacts on landscape carbon budgets, as demonstrated in this study. Changes in the fire regime may also result in a positive feedback on arctic carbon loss through interactions between burn severity and vegetation recovery. For example, higher severity fires may alter species composition from a tussock to a shrub-dominant system and result in more frequent arctic wildfires through increased fuel loads (Higuera et al. 2008). Consequently, understanding the short- and long-term consequences of burn severity on postfire carbon balance is critical in order to forecast future changes in the arctic carbon balance.

Acknowledgments

We thank the Toolik Lake Field Station for providing support and logistics and Jen Peters, Glenn Scott, and Jim Laundre for assistance in the field. This work was supported by NSF grants #0632139 (OPP-AON), #0808789 (OPP-ARCSS SGER), #0829285 (DEB-NEON SGER), and #0423385 (DEB-LTER) to the Marine Biological Laboratory.

Literature Cited

Baldocchi, D. D. 2008. 'Breathing' of the Terrestrial Biosphere: lessons learned from a global network of carbon dioxide flux measurement systems. Australian Journal of Botany 56:1–26.

Baldocchi, D. D., B. B. Hicks, and T. P. Meyers. 1988. Measuring biosphere–atmosphere exchanges of biologically related gases with micrometeorological methods. Ecology 69: 1331–1340.

Bergner, B., J. Johnstone, and K. K. Treseder. 2004. Experimental warming and burn severity alter soil CO_2 flux and soil functional groups in a recently burned boreal forest. Global Change Biology 10:1996–2004.

Bond-Lamberty, B., S. D. Peckham, D. E. Ahl, and S. T. Gower. 2007. Fire as the dominant driver of central Canadian boreal forest carbon balance. Nature 450:89–92.

Bond-Lamberty, B., C. K. Wang, and S. T. Gower. 2004. Net primary production and net ecosystem production of a boreal black spruce wildfire chronosequence. Global Change Biology 10:473–487.

Brais, S., P. David, and R. Ouimet. 2000. Impacts of wild fire severity and salvage harvesting on the nutrient balance of jack pine and black spruce boreal stands. Forest Ecology and Management 137:231–243.

Burba, G. G., D. K. Mcdermitt, A. Grelle, D. J. Anderson, and L. Xu. 2008. Addressing the influence of instrument surface heat exchange on the measurements of CO_2 flux from open-path gas analyzers. Global Change Biology 14:1–23.

Burke, R. A., R. G. Zepp, M. A. Tarr, W. L. Miller, and B. J. Stocks. 1997. Effect of fire on soil atmosphere exchange of methane and carbon dioxide in Canadian boreal forest sites. Journal of Geophysical Research–Atmospheres 102:29289–29300.

Davidson, E. A., I. A. Janssens, and Y. Luo. 2006. On the variability of respiration in terrestrial ecosystems: moving beyond Q_{10}. Global Change Biology 12:154–164.

Duffy, P. A., J. Epting, J. M. Graham, T. S. Rupp, and D. A. McGuire. 2007. Analysis of Alaskan burn severity patterns using remotely sensed data. International Journal of Wildland Fire 16:277–284.

Dyrness, C. T., and R. A. Norum. 1983. The effects of experimental fires on black spruce forest floors in interior Alaska. Canadian Journal of Forest Research 13:879–893.

Goetz, S. J., A. G. Bunn, G. J. Fiske, and R. A. Houghton. 2005. Satellite-observed photosynthetic trends across boreal North America associated with climate and fire disturbance. Proceedings of the National Academy of Sciences. [doi: 10.1073/pnas. 0506179102]

Goulden, M. L., G. C. Winston, A. M. S. McMillan, M. E. Litvak, E. L. Read, A. V. Rocha, and J. R. Elliot. 2006. An eddy covariance mesonet to measure the effect of forest age on land–atmosphere exchange. Global Change Biology 12:2146–2162.

Hargrove, W. W., F. M. Hoffman, and B. E. Law. 2003. New analysis reveals representativeness of the AmerifFlux network. Eos, Transactions of the American Geophysical Union 84:529.

Higuera, P. E., L. B. Brubaker, P. M. Anderson, T. A. Brown, A. T. Kennedy, and F. S. Hu. 2008. Frequent fires in ancient shrub tundra: implications of paleorecords for arctic environmental change. PloS ONE 3(3). ⟨e0001744.doi:10.1371/journal.pone.0001744⟩

Hudson, J. M. G., and G. H. R. Henry. 2009. Increased plant biomass in a High Arctic heath community from 1981 to 2008. Ecology 90:2657–2663.

Jiang, Z., A. R. Huete, K. Didan, and T. Miura. 2008. Development of a two-band enhanced vegetation index without a blue band. Remote Sensing of Environment 112:3833–3845.

Johnstone, J. F., and F. S. Chapin III. 2006. Effects of soil burn severity on postfire tree recruitment in boreal forest. Ecosystems 9:14–31.

Johnstone, J. F., T. N. Hollingsworth, F. S. Chapin, and M. C. Mack. 2010. Changes in fire regime break the legacy lock on successional trajectories in Alaskan boreal forest. Global Change Biology. *In press*. [doi: 10.111/j.1365-2486.2009.02051.x]

Jones, B. M., C. A. Kolden, R. Jandt, J. T. Abatzoglou, F. Urban, and C. D. Arp. 2009. Fire behavior, weather, and burn severity of the 2007 Anaktuvuk River Tundra Fire, North Slope, Alaska. Arctic, Antarctic, and Alpine Research 3:309–316.

Jung, M., M. Verstraete, N. Gobron, M. Reichstein, D. Papale, A. Bondeau, M. Robustelli, and B. Pinty. 2008. Diagnostic assessment of European gross primary production. Global Change Biology 14:2349–2364.

Kasischke, E. S., K. P. O'Neill, N. H. F. French, and L. L. Bourgeau-Chavez. 2000. Controls on patterns of biomass burning in Alaskan boreal forests. Pages 173–196 *in* E. S. Kasischke and B. J. Stocks, editors. Fire, climate change and carbon cycling in the boreal forest. Springer, New York, New York, USA.

Kasischke, E. S., and M. R. Turetsky. 2006. Recent changes in the fire regime across the North American boreal region—spatial and temporal patterns of burning across Canada and Alaska. Geophysical Research Letters 33 L09703. [doi: 10.1029/2006GL025677]

Keeley, J. E. 2006. Fire severity and plant age in postfire resprouting of woody plants in sage scrub and chaparral. Madroño 53:373–379.

Keeley, J. E. 2009. Fire intensity, fire severity and burn severity: a brief review and suggested usage. International Journal of Wildland Fire 18:116–126.

Key, C. H., and N. C. Benson. 1999. Measuring and remote sensing of burn severity. Page 284 *in* L. F. Neuenschwander and K. C. Ryan, editors. Proceedings of the Joint Fire Science Conference and Workshop. Volume II. Universiity of Idaho, Moscow, Idaho, USA.

Kim, J., Q. Guo, D. D. Baldocchi, M. Y. Leclerc, L. Xu, and H. P. Schmid. 2006. Upscaling fluxes from tower to landscape: overlaying flux footprints on high-resolution (IKONOS) images of vegetation cover. Agricultural and Forest Meteorology 136:132–146.

Kwon, H.-J., W. C. Oechel, R. C. Zulueta, and S. J. Hastings. 2006. Effects of climate variability on carbon sequestration among adjacent wet sedge tundra and moist tussock tundra ecosystems. Journal of Geophysical Research–Biogeosciences 111:G03014.

Lafleur, P. M., and E. R. Humphreys. 2008. Spring warming and carbon dioxide exchange over low arctic tundra in central Canada. Global Change Biology 12:740–756.

Liljedahl, A., L. Hinzman, R. Busey, and K. Yoshikawa. 2007. Physical short-term changes after a tussock tundra fire, Seward Peninsula, Alaska. Journal of Geophysical Research-Earth Surface, 112, F02S07. [doi: 10. 1029/2006JF000554]

Litvak, M., S. Miller, S. C. Wofsy, and M. Goulden. 2003. Effect of stand age on whole ecosystem CO_2 exchange in the Canadian boreal forest. Journal of Geophysical Research 108(D3):8225.

Lund, M., et al. 2009. Variability in exchange of CO_2 across 12 northern peatland and tundra sites. Global Change Biology, *in press*. [doi: 10.1111/j.1365-2486.2009.0214.x]

McMillan, A. M. S., and M. L. Goulden. 2008. Age-dependent variation in the biophysical properties of boreal forests. Global Biogeochemical Cycles 22:2 GB2019.

Meigs, G. W., D. C. Donato, J. L. Campbell, J. G. Martin, and B. E. Law. 2009. Forest fire impacts on carbon uptake, storage, and emission: the role of burn severity in Eastern Cascades, Oregon. Ecosystems 12:1245–1267.

Moncrieff, J. B., J. M. Massheder, H. de Bruin, J. Elbers, T. Friborg, B. Heusinkveld, P. Kabat, S. Scott, H. Sogaard, and A. Verhoef. 1997. A system to measure surface fluxes of momentum, sensible heat, water vapour and carbon dioxide. Journal of Hydrology 188–189:598–611.

Neary, D. G., C. C. Klopatek, L. F. DeBano, and P. F. Ffolliott. 1999. Fire effects on belowground sustainability: a review and synthesis. Forest Ecology and Management 122:51–71.

Oechel, W. C., and G. Vourlitis. 1997. Climate change in northern latitudes: alterations in ecosystem structure and function and effects on carbon sequestration. Pages 266–289 *in* W. C. Oechel, T. Callaghan, T. Gilmanov, J. I. Holten, B. Maxwell, U. Molau, and B. Sveinbjornsson, editors. Global change and arctic terrestrial ecosystems. Ecological Studies 124. Springer, New York, New York, USA.

O'Neill, K. P., E. S. Kasischke, and D. D. Richter. 2002. Environmental controls on soil CO_2 flux following fire in black spruce, white spruce, and aspen stands of interior Alaska. Canadian Journal of Forest Research 32:1525–1541.

Quaife, T., S. Quegan, M. Disney, P. Lewis, M. Lomas, and F. I. Woodward. 2008. Impact of land cover uncertainties on estimates of biospheric carbon fluxes. Global Biogeochemical Cycles 22 GB4016. [doi: 10.1029/2007GB003097]

Racine, C. E., L. A. Johnson, and L. A. Viereck. 1987. Patterns of vegetation recovery after tundra fires in northwestern Alaska, USA. Arctic and Alpine Research 4:461–469.

Rahman, A. F., D. A. Sims, V. D. Cordova, and B. Z. El-Masri. 2005. Potential of MODIS EVI and surface temperature for directly estimating per-pixel ecosystem C fluxes. Geophysical Research Letters 32:LI9404.

Raynolds, M. A., D. A. Walker, and H. A. Maier. 2005. Plant community-level mapping of arctic Alaska based on the Circumpolar Arctic Vegetation Map. Phytocoenologia 35: 821–848.

Reeve, N., and R. Toumi. 1999. Lightning activity as an indicator of climate change. Quarterly Journal of the Royal Meteorological Society 125:893–903.

Richardson, A. D., A. Y. Hollinger, J. D. Aber, S. V. Ollinger, and B. H. Braswell. 2007. Environmental variation is directly responsible for short- but not long-term variation in forest–atmosphere carbon exchange. Global Change Biology 13: 788–803.

Rocha, A. V., and M. L. Goulden. 2010. Drought legacies influence the long-term carbon balance of a freshwater marsh. Journal of Geophysical Research–Biogeosciences, *in press*. [10.1029/2009JG001215]

Rocha, A. V., and G. R. Shaver. 2009. Advantages of a two-band EVI calculated from solar and photosynthetically active radiation fluxes. Agricultural and Forest Meteorology 149: 1560–1563.

Roman, M. O., et al. 2009. The MODIS (Collection V005) BRDF/albedo product: assessment of spatial representativeness over forested landscapes. Remote Sensing of Environment 113:2476–2498.

Rowe, J. S. 1983. Concepts of fire effects on plant individuals and species. Pages 135–154 *in* R. W. Wein and D. A. MacLean, editors. The role of fire in northern circumpolar ecosystems. Wiley, Chichester, UK.

Ruimy, A., P. G. Jarvis, D. D. Baldocchi, and B. Saugier. 1995. CO_2 fluxes over plant canopies: a literature review. Advances in Ecological Research 26:1–68.

Schimel, J., and A. Granstrom. 1996. Fire severity and vegetation response in the Boreal Swedish forest. Ecology 77:1436–1450.

Schmid, H. P. 1997. Experimental design for flux measurements: matching scales of observations and fluxes. Agricultural and Forest Meteorology 87:179–200.

Shaver, G. R., L. E. Street, E. B. Rastetter, M. T. van Wijk, and M. Williams. 2007. Functional convergence in regulation of net CO_2 flux in heterogeneous tundra landscapes in Alaska and Sweden. Journal of Ecology 95:802–817.

Shelby, S. M. 1969. Standard mathematical tables: 17th edition. CRC, Boca Raton, Florida, USA.

Stoy, P. C., A. D. Richardson, D. D. Baldocchi, G. G. Katul, J. Stanovick, M. D. Mahecha, M. Reichstein, M. Detto, B. E. Law, G. Wohlfahrt, N. Arriga, J. Campos, J. H. McCaughey, L. Montagnani, K. T. Paw U, S. Sevanto, and M. Williams. 2009*a*. Biosphere–atmosphere exchange of CO_2 in relation to climate: a cross-biome analysis across multiple time scales. Biogeosciences 6:4095–4141.

Stoy, P. C., M. Williams, M. Disney, A. Prieto-Blanco, B. Huntley, R. Baxter, and P. Lewis. 2009*b*. Upscaling as ecological information transfer: a simple framework with application to Arctic ecosystem carbon exchange. Landscape Ecology 24:971–986.

Tape, K., M. Strum, and C. Racine. 2006. The evidence for shrub expansion in Northern Alaska and the Pan-Arctic. Global Change Biology 12:686–702.

Webb, E. K., G. I. Pearman, and R. Leuning. 1980. Correction of flux measurements for density effects due to heat and water vapour transfer. Quarterly Journal of Royal Meteorological Society 106:85–100.

Wein, R. W. 1976. Frequency and characteristics of arctic tundra fires. Arctic 29:213–222.

Wein, R. W., and L. C. Bliss. 1973. Changes in arctic *Eriophorum* tussock communities following fire. Ecology 54: 845–852.

Westerling, A. L., H. G. Hidalgo, D. R. Cayan, and T. W. Swetnam. 2006. Warming and earlier spring increases western U. S. forest wildfire activity. Science 313:940–943.

Wilson, K., et al. 2002. Energy balance closure at FLUXNET sites. Agricultural and Forest Meteorology 113:223–243.

Xiao, J., et al. 2008. Estimation of net ecosystem carbon exchange for the conterminous United States by combining MODIS and AmeriFlux data. Agricultural and Forest Meteorology 148:1827–1847.

Yang, F., A-X. Zhu, K. Ichii, M. A. White, H. Hashimoto, and R. R. Nemani. 2008. Assessing the representativeness of the Ameriflux network using MODIS and GOES data. Journal of Geophysical Research 113:G04036.